Synergistic cytotoxicity of radiation and oncolytic Lister strain vaccinia in $^{V600D/E}$BRAF mutant melanoma depends on JNK and TNF-α signalling

Kyula JN[1], Khan AA[1], Mansfield D[1], Karapanagiotou EM[1], McLaughlin M[1], Roulstone V[1], Zaidi, S[1], Pencavel T[1], Touchefeu Y[1], Seth R[1], Chen NG[2], Yu YA[2], Zhang Q[2], Melcher AA[3], Vile RG[3,4], Pandha HS[5], Ajaz M[5], Szalay AA[2], Harrington KJ[1]

[1]The Institute of Cancer Research, Divisions of Cancer Biology, Targeted Therapy Team, London, UK

[2]Genelux Corp, San Diego Science Center, San Diego, CA, USA

[3]Leeds Institute of Molecular Medicine, Leeds, UK

[4]Molecular Medicine Program, Mayo Clinic, Rochester, MN, USA

[5]Postgraduate Medical School, The University of Surrey, Guildford, UK

Address for correspondence:

Dr Joan N. Kyula
The Institute of Cancer Research
Division of Cancer Biology
Chester Beatty Laboratories
Targeted Therapy Team
237 Fulham Road
London SW3 6JB
Tel: 020 7352 8133
Fax: 020 7808 2235
e-mail: Joan.Kyula@icr.ac.uk

Keywords: oncolytic vaccinia, GLV-1h68, JNK, TNF-α, RT, apoptosis

Running title: Interaction between GLV-1h68 and RT in BRAF mutant melanoma

Abstract

Melanoma is an aggressive skin cancer that carries an extremely poor prognosis when local invasion, nodal spread or systemic metastasis has occurred. Recent advances in melanoma biology have revealed that RAS-RAF-MEK-ERK signalling plays a pivotal role in governing disease progression and treatment resistance. Proof-of-concept clinical studies have shown that direct BRAF inhibition yields impressive responses in advanced disease but these are short-lived as treatment resistance rapidly emerges. Therefore, there is a pressing need to develop new targeted strategies for BRAF mutant melanoma. As such, oncolytic viruses represent a promising cancer-specific approach with significant activity in melanoma.

This study investigated interactions between genetically-modified vaccinia virus (GLV-1h68) and radiotherapy in melanoma cell lines with BRAF mutant, Ras mutant or wild-type genotype. Pre-clinical studies revealed that GLV-1h68 combined with radiotherapy significantly increased cytotoxicity and apoptosis relative to either single agent in ^{V600D}BRAF/^{V600E}BRAF mutant melanoma *in vitro* and *in vivo*. The mechanism of enhanced cytotoxicity with GLV-1h68/radiation was independent of viral replication and due to attenuation of JNK, p38 and ERK MAPK phosphorylation specifically in BRAF mutant cells. Further studies showed that JNK pathway inhibition sensitized BRAF mutant cells to GLV-1h68-mediated cell death, mimicking the effect of radiation. GLV-1h68 infection activated MAPK signalling in ^{V600D}BRAF/^{V600E}BRAF mutant cell lines and this was associated with TNF-α secretion which, in turn, provided a prosurvival signal. Combination GLV-1h68/radiation (or GLV-1h68/JNK inhibition) caused abrogation of TNF-α secretion. These data provide a strong rationale for combining GLV-1h68 with irradiation in $^{V600D/E}$BRAF mutant tumors.

Introduction

Oncolytic viruses have the remarkable biological property of being able to replicate selectively in cancer cells, thus mediating tumor-selective cytotoxicity. A number of agents from a diverse range of viral families are currently in preclinical or clinical development. Indeed, herpes simplex virus type 1 (OncoVEX^{GM-CSF}), reovirus (Reolysin) and vaccinia virus (JX-594) have all reached late-stage, randomised clinical trials either as single agent therapies or in combination with cytotoxic chemotherapy. In addition, recent studies have highlighted the fact that combining oncolytic virotherapy with ionizing radiation may lead to synergistic anti-tumor efficacy and translational phase I/II clinical trials have been completed (1, 2). However, the reported complex effects of radiation on viral infectivity, replication, gene expression and cytotoxicity mean that detailed mechanistic preclinical studies are an essential prerequisite to trials of new oncolytic viral agents in combination with radiation.

Vaccinia virus strains are promising candidates for clinical application in treating cancer. They show a preference for replication in dividing cells and, indeed, are able to manipulate signalling through the mitogen-activated protein kinase (MAPK) pathway to create a cellular environment that is conducive to viral replication (3, 4). Tumor cell lines with constitutive activation of the MAPK pathway are likely to be susceptible to vaccinia virus-mediated oncolysis. In addition, ionising radiation can activate MAPK signalling and this may further increase viral replication in infected and irradiated tumor cells (5).

A Lister strain oncolytic vaccinia virus (GL-ONC1, Genelux GmbH) that has been attenuated by insertion of β-galactosidase, β-glucuronidase and *Renilla* luciferase-green fluorescent protein expression cassettes into the thymidine kinase (J2R), hemagglutinin

(A56R) and F14.5L loci is currently in phase I clinical evaluation. The anti-tumor activity of the equivalent, non-clinical grade virus (GLV-1h68) has been profiled in preclinical studies as part of the planning process for subsequent phase I and II clinical trials (6-12). These studies have included a detailed analysis of the combination of GLV-168 with radiation in malignant melanoma. This tumor type frequently presents with multiple cutaneous and subcutaneous deposits and represents an attractive model for early phase clinical studies of combinations of oncolytic viruses and radiation – not least because of its poor prognosis and relative radioresistance, but its accessibility for direct intratumoral injection and the potential to obtain repeated biopsies to measure pharmacodynamic markers (13). In addition, recent impressive results with the BRAF inhibitor, vemurafenib, suggest that malignant melanoma is an excellent scenario in which to test molecularly targeted agents (14).

In this report, we show that oncolytic vaccinia virus mediates synergistic toxicity with radiation in malignant melanoma, but only those that harbour ^{V600D}BRAF and ^{V600E}BRAF mutations. These data provide a strong rationale for testing this approach in other ^{V600D}BRAF or ^{V600E}BRAF mutant tumor types (e.g. colorectal, thyroid cancers) and support the clinical translation of this strategy.

Results

GLV-1h68 and radiation exert synergistic cytotoxicity in ^{V600E}BRAF mutant melanoma. The effect of GLV-1h68 infection in a panel of melanoma cell lines with wild-type BRAF/RAS, $^{V600D/E}$BRAF mutation or RAS (K- and N-) mutation was assessed 72 hours post infection by MTT (Supplementary Fig. S1 and Table S1). All melanoma cell lines were found to be sensitive to GLV-1h68 with the MeWo and PMWK wild-type cell lines being the most sensitive to GLV-1h68 with IC_{50} values of 0.5 and 0.05 MOI, respectively, by formal quantitative colorimetric assay. The WM17971 (K-RAS mutant) and D04 (N-RAS mutant) cell lines both had IC_{50} values of 1 MOI. The A375 ^{V600E}BRAF and WM266.4 ^{V600D}BRAF mutant cell lines were found to be less sensitive to GLV-1h68 with IC_{50} values of 2.5 MOI. We extended the panel of ^{V600E}BRAF mutant cell lines to include SKMel28 and Mel624, which both had IC_{50} values of 2.

We next determined the effect of combining GLV-1h68 and radiation (RT). Cells were irradiated to 1, 3 or 5 Gy fractions and 6 hours later were infected with GLV-1h68 at MOI ranging from 0.1-10 in 96-well plates for MTT assay (Fig. 1A) or a single fraction of 5 Gy and 6 hours later infected with GLV-1h68 at MOI between 0.001-1.0 in 24-well plates for SRB assay (Fig. 1B) and crystal violet staining (Supplementary Fig. S2A). Cell survival was determined 72 hours post-infection. The effect of RT alone did not cause a significant increase in cell death by MTT in all cell lines. There was a slight decrease in the A375 and WM266.4 BRAF mutant cell lines following radiation at 5 Gy as shown in the SRB assay but this was seen to be non-significant (Fig 1C). We found significantly greater cytotoxicity following combined GLV-1h68 and RT in the ^{V600E}BRAF and ^{V600D}BRAF mutant cell lines, A375 and WM266.4 respectively by MTT (Fig. 1A). To evaluate the level of synergy between RT and GLV-1h68, we used Bliss independence analysis as previously described (15-18). This methodology uses the formulae $E_{IND} = E_A + E_B - E_A \times E_B$ and $\Delta E = E_{OBS} - E_{IND}$ where: E_A and E_B are the fractional effect

of factors A and B, respectively; E_{IND} is the expected effect of an independent combination of factors; E_{OBS} is the observed effect of the combination. If ΔE and its 95% confidence interval (CI) are >0, synergy has been observed. If ΔE and its 95% CI are <0, antagonism has been observed. If ΔE and its 95% CI contain 0 then the combination is independent. The results from Bliss demonstrated a strong synergistic effect between GLV-1h68 and RT in the ^{V600E}BRAF and ^{V600D}BRAF cell lines, where ΔE was above 1 (Fig, 1B). There was, however, no synergistic effect in the MeWo and PMWK wild-type cell lines or the WM17971 (K-RAS mutant) and D04 (N-RAS mutant) cell lines. The SRB analysis showed enhanced cell kill in the BRAF mutant A375 and WM266.4 cell lines where p values were between 0.01 to <0.001 (Fig. 1C). This was further confirmed in the crystal violet assay (Supplementary Fig. S2) which showed no increase in cell kill with RT alone. All melanoma cell lines showed an increase in cell kill with increasing doses of GLV-1h68, Of note, the wild-type MeWo and PMWK cell lines formed bigger plaques with increasing GLV-1h68 infection while the A375 and WM266.4 BRAF mutant cell lines as well as the K-RAS WM1791 cells appeared more sensitive. Furthermore, the SRB assay quantitatively showed that all cell lines responded to increase in cell kill when treated with GLV-1h68 but the PMWK wild-type cell remained the most sensitive (Fig. 1C). More importantly, the quantitative SRB assay showed a significant increase in cell kill when RT and GLV-1h68 was combined in the A375 and WM266.4 BRAF mutant cell line (Fig. 1C).

In addition, colony formation assays were carried out to assess RT and GLV-1h68 interaction. MeWo, A375 and D04 cells were exposed to a single fraction of 2 or 5 Gy and surviving fraction determined. This was to assess the dose to take forward for combining radiation and GLV-1h68. We found all 3 cell lines had a very similar surviving fraction at 2 and 5 Gy (Fig. 1D and Supplementary Fig. S2B). In view of this, we used 2

Gy of radiation in combination with GLV-1h68 at an MOI of 0.01. Colony formation assays confirmed an increase in cell death due to combined virus and radiation therapy occurred in ^{V600E}BRAF mutant cells (Fig. 1E). Furthermore the other two ^{V600E}BRAF mutant cell lines, Mel624 and SKMel28 showed enhanced cytotoxicity when assayed for MTT, crystal violet and SRB assays (Supplementary Fig. S3). However, no significant increase in cytotoxicity was observed in the wild-type MeWo and PMWK or RAS mutant DO4 [N-RAS] and WM17971 [K-RAS] cell lines (Figure 1A-C and E).

Combined GLV-1h68 and RT enhances tumor growth delay in vivo and prolongs survival in A375 ^{V600E}BRAF mutant xenograft tumors. Subsequently, we assessed the in vivo relevance of the observations in Fig. 1 in A375 xenograft tumors. BALB CDI nude mice received subcutaneous injections of 5×10^6 A375 cells on the right flank. Once xenograft tumors had reached approximately 5 mm in diameter, the mice were randomly allocated into groups of 14 and treated with PBS alone, GLV-1h68 alone at 1×10^4 plaque forming units (PFU), radiation alone (6 Gy in 3 fractions) or a combination of 6 Gy in 3 fractions plus 1×10^4 PFU GLV-1h68. When radiation and GLV-1h68 were combined, the virus was given after the second fraction of radiation. GLV-1h68 and PBS were given by intratumoral injection. The treatment regimen is summarised in Fig. 2A. Four mice from each treatment group were culled after the end of the treatment on day 7 and tumors lysed and assessed for apoptosis by caspase 3-cleavage and TUNEL assay. Tumor size from the remaining 10 mice from each group was measured by Vernier callipers and volumes were plotted as soon as treatment began as shown in Fig. 2B. Tumors in all groups were slow to propagate up until Day 30 after which point a loss of growth delay was observed in control, radiation and virus alone groups. Combined treatment with GLV-1h68 and RT attenuated tumor growth compared to either RT or GLV-1h68 alone.

We performed multiple Mann-Whitney U-tests at serial time points after day 45, which demonstrated that statistically significant differences between groups persisted until the end of the experiment (Fig. 2C). In addition, survival analysis showed that mice treated with a combination of GLV-1h68 and RT took significantly longer to reach the experiment endpoint (tumor > 15 mm diameter) than mice treated with either GLV-1h68 or RT alone with a p value of 0.0099 (Fig. 2D). Consistent with the tumor growth data, Western blotting analysis showed an increase in caspase 3 cleavage when RT and GLV-1h68 were combined (Fig. 2E). Furthermore, TUNEL assay confirmed enhanced apoptosis with the combined RT and GLV-1h68 compared to GLV-1h68 or RT treatment alone (Fig. 2F).

RT does not enhance GLV-1h68 viral replication in $^{V600D/E}$BRAF mutant melanoma cells. To investigate whether the observed synergy between radiation and GLV-1h68 in $^{V600D/E}$BRAF mutant cells was due to increased viral replication, viral growth curves and quantitative PCR assays were performed. Cells were irradiated with a single 5 Gy fraction and 6 hours later were infected with GLV-1h68 at MOI of 1.0 (for measuring viral growth curves) or 0.01-1.0 (for A21L expression) and viral replication was assessed at various time points for the viral growth curve and 48 hour post-infection for A21L expression. The data from the viral growth curves as determined by $TCID_{50}$ or total viral titers quantified by plaque assays on confluent CV-1 cells (Fig. 3A & B respectively) and viral A21L expression measured by PCR (Fig. 3C) clearly showed that the enhanced cell kill was not due to an increase in viral replication when the cells were irradiated. Surprisingly, there was a clear reduction in viral replication in $^{V600D/E}$BRAF mutant cell lines following irradiation, while no change was noted in the wild-type or RAS mutant cells.

Having shown that viral replication was not responsible for increased cell death in irradiated $^{V600D/E}$BRAF mutant cells, we used a human phospho-kinase array to investigate what proteins might be involved in mediating the interaction between radiation and GLV-1h68 in MeWo and A375 melanoma cell lines (Fig. 4A). Of note, there was an increase in p38, JNK and ERK phosphorylation in both the A375 (^{V600E}BRAF mutant) cell lines following GLV-1h68 infection. However, following RT the phosphorylation of p38, JNK and ERK was abrogated in the A375 ^{V600E}BRAF mutant cell line. In the MeWo cells, there was a substantial increase in JNK phosphorylation following GLV-1h68 infection but little or no change in p38 or ERK phosphorylation, with RT having no effect on GLV-1h68 induced JNK phosphorylation (Fig. 4A). We then confirmed the results of the kinase array of both MeWo and A375 cells using Western blotting as shown in Fig. 4B. Our Western analysis in the A375 cells was consistent with the data from the Kinase Array where we saw abrogation of GLV-1h68 induced phosphorylation of p38, JNK and ERK following RT. The Western analysis for the MeWo cells were slightly different from that seen in the Kinase Array as GLV-1h68 showed a clear increase in p38 and ERK phosphorylation. Based on the consistent signal on the Kinase array and Western Blot, we chose to focus on the effect of GLV-1h68 and RT on the JNK pathway.

Inhibition of the JNK pathway following irradiation results in increased cell death.

To assess the role of JNK in regulating GLV-1h68 and RT-induced cell death, we carried out Western blotting analysis (Fig. 4C) to assess caspase 3 cleavage, a marker of apoptosis. We found modest or no increase in caspase 3 cleavage following GLV-1h68 infection in WM266.4 ^{V600D}BRAF, A375 ^{V600E}BRAF mutant cell lines. When GLV-1h68 was combined with RT, there was a marked increase in caspase 3 cleavage compared to GLV-1h68 or RT alone. When JNK phosphorylation status was assessed, we found

that RT abrogated GLV-1h68-induced JNK phosphorylation in the $^{V600D/E}$BRAF mutant cell line. In addition the other two ^{V600E}BRAF mutant cell lines, Mel624 and SKMel28 showed a similar pattern where there was a marked increase in caspase 3 cleavage when GLV-1h68 was combined with RT. This correlated with a loss of GLV-1h68 induced JNK phosphorylation (Supplementary Fig. S4B). Meanwhile, an increase in caspase 3 cleavage was seen following GLV-1h68 infection in wild-type (PMWK and MeWo) and N- and K-RAS mutant (DO4 and WM17971 respectively) cell lines (Fig. 4C). This was associated with an increase in JNK phosphorylation. In these cells, no increase in caspase 3 cleavage was seen following GLV-1h68 and RT treatment while JNK phosphorylation remained unchanged.

We next determined if the JNK pathway played a role in the mechanism of GLV-1h68 and RT-induced cell death in $^{V600D/E}$BRAF mutant cells, we used a specific JNK inhibitor (SP600125) in an attempt to mimic the effect of RT on GLV-1h68-induced cytotoxicity. Western analysis showed an increase in caspase 3 cleavage in A375 cells following RT and GLV-1h68 infection, as previously shown (Fig. 5A upper panel). Caspase 3 cleavage was also increased following GLV-1h68 infection combined with JNK inhibition therefore suggesting that JNK abrogation played a role in enhancing GLV-1h68 and RT-induced cell death. Similar results were obtained for 3 other BRAF mutants: WM266.4, Mel624 and SKMel28 cell lines (Fig. 6A). In addition, 2 other RAS mutant cell lines; D04 and WM1791 and wild-type MeWo cells were tested and showed no effect (Fig. 5A and 6A). Furthermore, JNK gene silencing by siRNA mimicked the results observed from the SP600125 inhibitor showing enhanced caspase cleavage when GLV-1h68 was combined with JNK siRNA in A375 cells but not in MeWo or D04 cells (Fig. 5A lower panel).

Subsequently, by using SRB assay, we found that a combination of SP600125 and GLV-1h68 resulted in increased cell death compared to either agent alone in the A375,

WM266.4, Mel624 and SKMel28 $^{V600D/E}$BRAF mutant cell lines (Fig. 5B and Fig. 6B) with similar cell kill observed for GLV-1h68 combined with either SP600125 or RT. However, there was no enhanced cell death in wild-type MeWo cell lines or N-and K-RAS D04 and WM1791 cell lines respectively when SP600125 was combined with GLV-1h68 - in keeping with the data for GLV-1h68 combined with RT (Fig. 5B and Fig. 6C). Crystal violet staining was also carried out and confirmed the response patterns described in the SRB assay (Supplementary Fig. S5). Additionally, using the SRB assay, we found that gene silencing of JNK in combination with GLV-1h68 enhanced cell death compared to either agent alone in A375 ^{V600E}BRAF mutant cell line (Fig 5B, lower panel). However there was no increase in cell death in either wild type MeWo or D04 N-RAS mutant cell lines following JNK silencing and GLV-1h68 infection. As was the case for GLV-1h68 in combination with radiation, GLV-1h68 in combination with SP600125 attenuated viral replication in $^{V600D/E}$BRAF mutant, but not wild-type or RAS mutant cell lines (Fig. 5C, 5D and Fig. 6C).

RT or JNK inhibition reduces TNF-α secretion following GLV-1h68 infection in $^{V600D/E}$BRAF mutant melanoma cells only.

TNF-α is a pleiotropic cytokine that plays a central role in inflammation and apoptosis (19). Paradoxically, it has previously been shown to act as a survival signal in ^{V600D}BRAF and ^{V600E}BRAF mutant melanoma cell lines where it prevented MEK inhibitor-induced cell death(20). Using a human TNF-α ELISA, we were able to show that TNF-α secretion was increased after GLV-1h68 infection in both $^{V600D/E}$BRAF mutant and wild-type melanoma cell lines. Following RT, TNF-α secretion was reduced in A375 ^{V600E}BRAF and WM266.4 ^{V600D}BRAF mutant cell lines, but no reduction was seen in wild-type cells (Fig. 7A). To test if the abrogation of GLV-1h68-induced TNF-α secretion in ^{V600E}BRAF mutant cell lines was JNK mediated, we used the specific JNK inhibitor, SP600125 and TNF-α

monoclonal antibody (mAb). We found that GLV-1h68-induced TNF-α secretion was abrogated by SP600125 in A375 ^{V600E}BRAF mutant, but not wild-type MeWo, cells (Fig. 7B). These findings mirror the effects seen with RT and SP600125. Using Western blotting analysis to detect caspase 3 cleavage, crystal violet staining and SRB assay to measure cell death, we found that a combination of TNF-α mAb and GLV-1h68 resulted in increased cell death compared to either agent alone in the A375 ^{V600E}BRAF mutant cell lines compared to wild type MeWo cells (Fig. 7C, D and E respectively).

Discussion

Metastatic malignant melanoma (MMM) is a highly aggressive tumor that is largely refractory to conventional anti-cancer chemotherapy (21-24). It is classically regarded as relatively resistant to radiation therapy (13). As a result, for many years, most oncologists have viewed MMM nihilistically as an essentially untreatable disease. However, recent studies have shown that MMM can be divided into specific molecular pathological subtypes that may be amenable to specific targeted therapies. For example, the finding that approximately 50% of melanomas harbour oncogenic BRAF mutations has driven drug discovery programmes that have generated potent, selective inhibitors that are active against ^{V600E}BRAF mutant tumor cells (25-27). These agents have yielded dramatic results in clinical trials in patients with ^{V600E}BRAF mutant melanoma (28, 29). The BRIM-3 phase III study recently reported response rates of 48% for PLX4032 (vemurafenib) versus 5% for the standard-of-care (dacarbazine) in patients with ^{V600E}BRAF mutant melanoma (14). These data translated to a 20% advantage for vemurafenib in terms of overall survival at 6 months. However, therapeutic responses were usually short-lived (less than one year) and frequently associated with aggressive disease recurrence. These observations highlight the need for continued research effort

in to novel therapies for BRAF mutant melanoma. As a note of caution, however, the importance of a detailed understanding of the molecular pathology of MMM was underlined in preclinical work that showed that, in BRAF wild-type tumor cells, the use of a BRAF inhibitor can activate signalling through BRAF-CRAF dimerisation and, as a result, may accelerate tumor growth (27). Therefore, future development of specific targeted therapies for MMM must include a detailed analysis of the various genetic backgrounds of this disease.

In the context of this evolving understanding of the molecular pathology of MMM, we have assessed the combined effect of GLV-1h68 and radiation in a panel of melanoma cell lines of varying genetic backgrounds (^{V600D}BRAF mutant, ^{V600E}BRAF mutant, K-RAS mutant, N-RAS mutant and wild-type for BRAF, K-RAS and N-RAS). We hypothesised that constitutive activation of JNK signalling would render RAS or BRAF mutant melanoma cell lines highly susceptible to vaccinia viral replication and oncolysis. Furthermore, we posited that radiation-induced activation of JNK signalling would further enhance replicative viral cytotoxicity in all genetic backgrounds.

Contrary to expectations, BRAF/RAS wild-type melanoma cell lines were more sensitive to GLV-1h68 than the BRAF or RAS mutants (Supplementary Fig. 1A) and only the 4 $^{V600D/E}$BRAF mutant cell lines showed enhanced cell death when GLV-1h68 was combined with radiation in vitro (Fig. 1A-D and Supplementary Fig. S2) and in vivo (Fig. 2). These findings suggested a complex combinatorial interaction between vaccinia virus and radiation in melanoma cell lines that is governed by the underlying molecular pathology of the disease. Therefore, in subsequent experiments we sought to uncover the mechanisms underpinning the differential effects of vaccinia virus and radiation in $^{V600D/E}$BRAF mutant, compared with RAS mutant or BRAF/RAS wild-type, melanoma cells.

In line with the received wisdom that oncolytic viruses kill by viral replication, we hypothesised that the increased cell death in $^{V600D/E}$BRAF mutant melanoma cells treated with vaccinia virus and radiation would be explicable in terms of enhanced viral replication. Certainly, a number of previous studies with different viruses have reported increased viral replication linked to enhanced lytic cytotoxicity following combination treatment with either radiation or cytotoxic chemotherapy (30-32). However, others have reported no change or a reduction in viral replication in combination regimens with radiation or chemotherapy (23, 33-37). Our data clearly demonstrate by both viral plaque assay and quantitative PCR that the enhanced cytotoxicity of the combined treatment in $^{V600D/E}$BRAF mutant cells was not due to increased viral replication. Paradoxically, the increased levels of cell death were associated with a definite decrease in viral replication in $^{V600D/E}$BRAF mutant cells (Fig. 3). In contrast, there was no difference in viral replication in RAS mutant or wild-type melanoma cell lines.

Having established that the synergistic effect of the combined treatment in $^{V600D/E}$BRAF mutant cells was not due to increased viral replication, we examined the activity of intracellular signalling pathways in response to viral infection, irradiation and the combination of infection and irradiation. Vaccinia virus is known to manipulate host-signalling pathways, such as MAPK (3) and Akt (38, 39) pathways, to enhance viral replication. Using a kinase array, we showed that infection with GLV-1h68 activated JNK pathways in both ^{V600E}BRAF mutant and BRAF/RAS wild-type cells. Critically, following irradiation, JNK signalling was abrogated in ^{V600E}BRAF mutant A375 cells, but unaltered or further increased in wild-type MeWo cells (Fig. 4A). This observation may, in part, explain the reduced viral replication seen after irradiation in $^{V600D/E}$BRAF mutant cells. Our data suggest that the abrogation of p-JNK signalling in $^{V600D/E}$BRAF mutant cells is associated with reduced vaccinia virus replication but increased levels of apoptosis, with the net effect being synergistic cytotoxicity.

We subsequently demonstrated that pharmacological inhibition of JNK phosphorylation recapitulated the effects of RT in terms of cytotoxicity (Fig. 5B and Fig. 6B), viral replication (Fig. 5C, D and Fig 6C) and caspase cleavage (Fig. 5A and Fig 6A). These findings suggest that RT-induced inhibition of JNK phosphorylation in $^{V600D/E}$BRAF mutant melanoma cells plays a key role in mediating the differential effects of RT in the different genetic backgrounds of melanoma.

Having seen differential signalling in JNK cascades in $^{V600D/E}$BRAF mutant and wild-type cells following the combination of vaccinia virus and RT, we focussed on understanding potential causes and effects of these changes. Previous studies have shown a role for TNF-α signalling in the tumor microenvironment in *de novo* skin carcinogenesis (40) and TNF-α has been shown to activate MAPK (p38MAPK, ERK and JNK) pathways (41, 42). Therefore, we investigated TNF-α signalling following GLV-1h68 infection alone and in combination with radiation. These studies revealed that melanoma cells harbouring a $^{V600D/E}$BRAF mutation were relatively resistant to GLV-1h68-induced cell death and that this was associated with TNF-α secretion and activation of p38MAPK, ERK and JNK. However, following irradiation, GLV-1h68-induced TNF-α secretion was significantly reduced in ^{V600E}BRAF mutant, but not wild-type, cells with co-ordinate reduction in p38MAPK, ERK and JNK signalling and enhanced cytotoxicity. These data are in line with previous work from other laboratories that have shown that TNF-α can function as a survival signal in $^{V600D/E}$BRAF mutant melanoma cells lines (17). Therefore, we hypothesize that inhibition of GLV-1h68 induced TNF-α and JNK pathways by RT or pharmacological (SP600125) means removes essential survival signals and results in an increase in $^{V600D/E}$BRAF mutant cell death (Fig. 7D).

In summary, our pre-clinical studies have provided a strong rationale for clinical translation of GLV-1h68 in combination with irradiation in $^{V600D/E}$BRAF mutant cells, while

also supporting the use of GLV-1h68 monotherapy in RAS mutant and BRAF/RAS wild-type melanoma. We are currently attempting to dissect how and why RT regulates vaccinia induced TNF-α/JNK survival pathways in $^{V600D/E}$BRAF mutant, but not wild type or Ras mutant cells and how this mediates enhanced cell death. In addition, we are further characterising other signalling alterations that were identified following GLV-1h68 and RT treatment, in particular the p38 MAPK and ERK pathways.

Materials & Methods

Cell lines. Melanoma cell lines of known genetic background were obtained from Prof. Richard Marais (The Paterson Institute of Cancer Research). The following cell lines were used: A375 Mel624, SKMel28 (all ^{V600E}BRAF mutant), WM266.4 (^{V600D}BRAF mutant), Mewo and PWMK (wild type RAS and BRAF), D04 (N-RAS mutant) and WM17971 (K-RAS mutant). All the cell lines were authenticated by using short tandem repeat (STR) profiling carried out by Bio-Synthesis Inc (Texas, USA) within the last 6 months. For simplicity, throughout the rest of this manuscript, BRAF mutant cell lines, which are either ^{V600D} BRAF or ^{V600E}BRAF mutant will be referred to as $^{V600D/E}$BRAF mutant. Cells were cultured in DMEM. Media was supplemented with 5% (v/v) FCS, 1% (v/v) glutamine, and 0.5% (v/v) penicillin/streptomycin.

Oncolytic vaccinia (GLV-1h68). GLV-1h68 is a genetically-engineered Lister strain vaccinia that was generated by inserting three expression cassettes [encoding *Renilla* luciferase-*Aequorea* green fluorescent protein (GFP) fusion protein, β-galactosidase (β-gal), and β-glucuronidase] into the *F14.5L, J2R, and A56R* loci of the LIVP (Lister strain from the Institute of Viral Preparations, Moscow, Russia) strain viral genome, respectively.

3-(4,5-dimethylthiazol-2-yl)-2,5-diphenyltetrazolium bromide assay. Cell viability was quantified using a 3-(4,5-dimethylthiazol-2-yl)-2,5-diphenyltetrazolium bromide (MTT) assay. Briefly 20 μl MTT (thiazolyl blue; Sigma-Aldrich) at 5 mg/ml in PBS was added to treated cells in a 96-well plate. After 4 hours incubation at 37°C, crystals were solubilised in DMSO and absorbance was measured at 570 nm on a SpectraMax 384 plate reader (Molecular Devices).

Crystal violet and sulforhodamine B assays. Cell viability was quantified by staining either with crystal violet (Sigma-Aldrich) at 0.2% (w/v) in a 7% (v/v) solution of ethanol/PBS or 10% trichloroacetic acid (TCA) and stained with sulforhodamine B (SRB). The crystal violet stained images of the plate were captured on a Microtek ScanMaker 8700 (Microtek International Ltd) while the SRB stained cells were diluted with 1mM TRIS and absorbance was measured at 570 nm on a SpectraMax 384 plate reader.

Clonogenic assays. For studies to determine the effect of radiation (RT) at 0, 2 and 5Gy, melanoma cells were plated on a six-well plate (density was dependent on plating efficiency), and 24 hours later radiation was delivered. After 10 to 14 days, colonies were fixed, stained, and counted. Cell survival was determined by normalization to the untreated control after correcting for the plating efficiency. For studies involving GLV-1h68 in combination with RT, cells were plated at 5×10^5 in a T25 flask. The next day, cells were irradiated 2Gy and 6 hours later infected with GLV-1h68 at a multiplicity of infection (MOI) of 0.03. Forty-eight hours post-treatment, cells were washed in PBS, trypsinized and counted using a haemocytometer. Cells were then plated into 6-well

dishes at 400-800 cells/well. After 10-14 days plates were stained with 0.2% crystal violet in 7% ethanol 10-14 days later and the plates containing the colonies scanned.

One step growth curve assays. Titers of GLV-1h68 in infected melanoma cells (with or without RT) were determined. Briefly, melanoma cells were seeded in 24 well plates at a density of $2X10^5$ cells/well and infected with GLV-1h68 at an MOI of 1. The cells were harvested and the supernatants were collected at 4, 24, 48 and 72 hours post-infection in triplicate. After three freeze-thaw cycles between −80°C and room temperatures, the resulting lysates or viral suspensions were diluted in 10-fold series and used to infect CV-1 cells. Viral titers were determined by limited dilution using he $TCID_{50}$/method.

Viral plaque assays (VPA) to determine viral titres. Melanoma cells were plated at 2×10^5 per well in 24-well plates. Culture plates were irradiated the next day at 5 Gy and infected with GLV-1h68 at an MOI of 1. Supernatant from each well was collected at 48 hours post-infection and the viral plaques from the infected cells released by 3 freeze-thaw cycles. CV-1 cells were grown to confluence on 24 well plates. Supernatants were thawed, and serial dilutions incubated on the CV-1 cells for 4 hours. Wells were washed with media and incubated with fresh media. After 48 hours of incubation, virus detection was carried out on the cell monolayers. Briefly, cells were washed with PBS, fixed with 0.2% Glutaraldehyde/2% formaldehyde for 5 minutes, and thereafter washed with PBS. Cells were stained for 4 hours in X-galactosidase (0.6 mg/ml) in a solution of 5 mM $K_4Fe(CN)_6$, 5 mM $K_3Fe(CN)_6$, and 2 mM $MgCl_2$ and the viral plaques counted and the viral titers determined. In addition, viral plaques from MeWo and A375 cell lines were also captured on a Microtek ScanMaker 8700 (Microtek International Ltd) or examined by microscopy (x20).

A21L expression. qPCR using the Genelux GL-LC1 VV-A21L kit was used for semi-quantitative detection of the vaccinia A21L gene. DNA was prepared from the media of melanoma cells following infection with GLV-1h68 +/- irradiation at 48 hours. A21L specific primers were used (forward: 5′-CGT AAA CTA CAA ACG TCT AAA CAA GAA-3′ and reverse: 5′-CCT GGT ATA TCG TCT CTA TCT TTA TCA C-3′). The 18S rRNA of human/rat genomic DNA (18S) was used as a reference.

Kinase array. The activity of 46 kinase phosphorylation sites was assessed using an antibody-based array from R&D Systems. Cell lysates were obtained from A375 or MeWo cells exposed to the following experimental conditions: untreated (no virus, no radiation); virus only (GLV-1h68 virus infected, no radiation); radiation only (no virus, irradiated to 5 Gy); and combined virus and radiation (infected with GLV-1h68 and irradiated to 5 Gy).

Small interfering RNA transfections. Scramble control and JNK1/2 siRNA small interfering RNAs (siRNA) were obtained from Dharmacon. MeWo, A375 and D04 cells were seeded out in the appropriate media without penicillin-streptomycin. Twenty-four hours after seeding, siRNA transfections were done on subconfluent cells incubated in unsupplemented OptiMEM using the Lipofectamine reagent (Invitrogen) according to the manufacturer's instructions. After 4 hours, 3X growth medium was added to the media. Cells were then infected with GLV-1h68 (MOI of 0.1) for 72 hours and the lysates collected for Western analysis or assessed for cell death by SRB assay.

Western blotting. Cells were plated at 0.5×10^6 in 60 mm dishes. Following various treatments, cells were harvested in ice-cold PBS, pelleted and resuspended in radioimmunoprecipitation assay buffer [50 mM Tris (pH 7.5), 150 mM NaCl, 1% NP40,

0.5% sodium deoxycholate, and 0.1% SDS] with protease inhibitors (Roche Diagnostics GmbH, Mannheim, Germany), 1 mM sodium orthovanadate (Sigma), and 10 mM sodium fluoride. Cells were then lysed by snap freezing on dry ice and then allowing the lysate to thaw on ice for 10 minutes. The lysate was then centrifuged at 13,200 rpm/4°C for 20 minutes to remove cell debris. Protein concentration was determined using the BCA protein assay reagent (Pierce, Rockford, IL). 30 μg of each protein sample were resolved on SDS-polyacrylamide gels (10-12%) and transferred to a polyvinylidene difluoride Hybond-P membrane (Amersham, Buckinghamshire, United Kingdom). Immunodetections were performed using anti-phosphorylated JNK (Thr 183/Tyr 185, Cell Signaling), anti-phosphorylated p38 MAPK (Thr 180/Tyr 182, Cell Signaling), anti-phosphorylated p44/42 ERK MAPK (Thr 202/Tyr 204, Cell Signaling) and caspase 3 (Cell Signaling) rabbit polyclonal antibody in conjunction with a horseradish peroxidase (HRP)-conjugated anti-rabbit secondary antibody (GE-Healthcare). Equal loading was assessed using α-tubulin (Sigma Aldrich) or glyceraldehyde-3-phosphate dehydrogenase-GAPDH (Biogenesis) mouse monoclonal primary antibodies. The Super Signal chemiluminescent system (Pierce) or Immobilon Western chemiluminescent HRP substrate (Millipore) were used for detection.

In vivo studies. A375 tumors were established in female CD1 nude mice by subcutaneous (s.c) injection of 5×10^6 cells suspended in 100 μL PBS in the right flank. Once xenografts were established and reached approximately 5 mm in diameter, mice were randomly allocated to treatment groups (14 mice per group) before beginning therapy. Irradiation of mice was carried out as previously described (32). Briefly, mice received an i.p. injection of 100 μL of a 1:1:4 mixture of Hypnorm (0.315 mg/mL fentanyl citrate and 10 mg/mL fluanisone; Janssen-Cilag Ltd.), Hypnovel (5 mg/mL midazolam;

Roche Products Ltd.), and water for injection BP (Fresenius Health Care Group) prior to irradiation. Control animals were also anesthetized in the same way. Anesthetized animals were positioned in an irradiation jig with the s.c. tumors exposed under an aperture in a 3-mm lead sheet that shielded the rest of the body. Following irradiation, to limit hypothermia to a minimum, animals were wrapped in toweling jackets until they recovered consciousness (approximately 30-60 min). Local fractionated radiation treatment of the tumor consisted of a total dose of 6 Gy in 3 fractions over 5 days (Figure 2). GLV-1h68 was administered by intra-tumoral injection 1 hour before the 2^{nd} fraction of radiation dose. 4 mice from each group were sacrificed after 7 days treatment and tumors harvested for Caspase 3 cleavage (3 mice/group) and TUNEL staining (1 mouse/group). Tumors from the remaining mice (10 mice per group) were measured twice weekly in two dimensions using Vernier callipers and the volume estimated using the formula ($width^2 \times length$)/2. As per our institutions animal licensing regulations humane endpoint was defined as a tumor diameter greater than 15mm in any dimension.

TUNEL Assay and Caspase 3 cleavage. For in vivo analysis of apoptosis, tumors were harvested from mice 7 days after treatment and analysed for TUNEL staining (1 mouse per group) and by Western blot analysis for activated caspase 3 (3 mice per group). Tumors harvested for immunohistochemistry staining were fixed in 10% formalin for 24 hours and then transferred to PBS and stored at 4°C until analysed. Tumors for Western analysis were snap-frozen and homogenised for 2 cycles of 10 seconds in RIPA buffer. Samples were then centrifuged at 13,000 rpm for 20 minutes at 4ºC and the supernatant transferred to a fresh tube. Western analysis was carried out as described previously (in Western blotting methods above).

Statistical analysis. Comparisons between groups were done using the two way ANOVA (in vitro analysis) or a Mann-Whitney U test (in vivo analysis). Survival curves were estimated using the Kaplan-Meier method, and significance was assessed using the log-rank test. P values <0.05 were considered to be statistically significant (*, $P < 0.05$; **, $P < 0.01$; ***, $P < 0.005$). Synergy interactions between different treatments (e.g. GLV-1h68 and radiation) were tested by standard mathematical analyses of data from MTT assays. Specifically, the presence (or absence) of synergy was quantified by Bliss Independence Analysis(15-18) described by the formulae $E_{IND} = E_A + E_B - E_A \times E_B$ and $\Delta E = E_{OBS} - E_{IND}$ where: E_A and E_B are the fractional effect of factors A and B, respectively; E_{IND} is the expected effect of an independent combination of factors; E_{OBS} is the observed effect of the combination. If ΔE and its 95% confidence interval (CI) are >0 synergy has been observed. If ΔE and its 95% CI are <0 antagonism has been observed. If ΔE and its 95% CI contain 0 then the combination is independent. All plots were generated using Prism GraphPad software.

Conflict of interest

Aladar Szalay is president and a shareholder of GeneLux corporation. Kevin Harrington receives funding from GeneLux corporation in support of laboratory research.

Acknowledgments

We would like to thank Dr Khin Thway and Dr Michelle Wilkinson for their assistance with data acquisition and analysis.

References

1. Harrington KJ, Karapanagiotou EM, Roulstone V, Twigger KR, White CL, Vidal L, et al. Two-stage phase I dose-escalation study of intratumoral reovirus type 3 dearing and palliative radiotherapy in patients with advanced cancers. Clin Cancer Res. 2010;16(11):3067-77. Epub 2010/05/21.
2. Comins C, Spicer J, Protheroe A, Roulstone V, Twigger K, White CM, et al. REO-10: a phase I study of intravenous reovirus and docetaxel in patients with advanced cancer. Clin Cancer Res. 2010;16(22):5564-72. Epub 2010/10/12.
3. Andrade AA, Silva PN, Pereira AC, De Sousa LP, Ferreira PC, Gazzinelli RT, et al. The vaccinia virus-stimulated mitogen-activated protein kinase (MAPK) pathway is required for virus multiplication. Biochem J. 2004;381(Pt 2):437-46. Epub 2004/03/18.
4. de Magalhaes JC, Andrade AA, Silva PN, Sousa LP, Ropert C, Ferreira PC, et al. A mitogenic signal triggered at an early stage of vaccinia virus infection: implication of MEK/ERK and protein kinase A in virus multiplication. J Biol Chem. 2001;276(42):38353-60. Epub 2001/07/19.
5. Dent P, Yacoub A, Fisher PB, Hagan MP, Grant S. MAPK pathways in radiation responses. Oncogene. 2003;22(37):5885-96. Epub 2003/08/30.
6. Ascierto ML, Worschech A, Yu Z, Adams S, Reinboth J, Chen NG, et al. Permissivity of the NCI-60 cancer cell lines to oncolytic Vaccinia Virus GLV-1h68. BMC Cancer. 2011;11:451. Epub 2011/10/21.
7. Yu YA, Galanis C, Woo Y, Chen N, Zhang Q, Fong Y, et al. Regression of human pancreatic tumor xenografts in mice after a single systemic injection of recombinant vaccinia virus GLV-1h68. Molecular cancer therapeutics. 2009;8(1):141-51. Epub 2009/01/14.
8. Gentschev I, Stritzker J, Hofmann E, Weibel S, Yu YA, Chen N, et al. Use of an oncolytic vaccinia virus for the treatment of canine breast cancer in nude mice: preclinical development of a therapeutic agent. Cancer Gene Ther. 2009;16(4):320-8. Epub 2008/10/25.
9. Yu Z, Li S, Brader P, Chen N, Yu YA, Zhang Q, et al. Oncolytic vaccinia therapy of squamous cell carcinoma. Mol Cancer. 2009;8:45. Epub 2009/07/08.
10. Lin SF, Price DL, Chen CH, Brader P, Li S, Gonzalez L, et al. Oncolytic vaccinia virotherapy of anaplastic thyroid cancer in vivo. J Clin Endocrinol Metab. 2008;93(11):4403-7. Epub 2008/08/14.
11. Kelly KJ, Woo Y, Brader P, Yu Z, Riedl C, Lin SF, et al. Novel oncolytic agent GLV-1h68 is effective against malignant pleural mesothelioma. Hum Gene Ther. 2008;19(8):774-82. Epub 2008/08/30.

12. Zhang Q, Yu YA, Wang E, Chen N, Danner RL, Munson PJ, et al. Eradication of solid human breast tumors in nude mice with an intravenously injected light-emitting oncolytic vaccinia virus. Cancer Res. 2007;67(20):10038-46. Epub 2007/10/19.
13. Khan N, Khan MK, Almasan A, Singh AD, Macklis R. The evolving role of radiation therapy in the management of malignant melanoma. Int J Radiat Oncol Biol Phys. 2011;80(3):645-54. Epub 2011/04/15.
14. Chapman PB, Hauschild A, Robert C, Haanen JB, Ascierto P, Larkin J, et al. Improved survival with vemurafenib in melanoma with BRAF V600E mutation. N Engl J Med. 2011;364(26):2507-16. Epub 2011/06/07.
15. Mansfield D, Pencavel T, Kyula JN, Zaidi S, Roulstone V, Thway K, et al. Oncolytic Vaccinia virus and radiotherapy in head and neck cancer. Oral oncology. 2012. Epub 2012/08/29.
16. Buck E, Eyzaguirre A, Brown E, Petti F, McCormack S, Haley JD, et al. Rapamycin synergizes with the epidermal growth factor receptor inhibitor erlotinib in non-small-cell lung, pancreatic, colon, and breast tumors. Molecular cancer therapeutics. 2006;5(11):2676-84. Epub 2006/11/24.
17. Greco WR, Bravo G, Parsons JC. The search for synergy: a critical review from a response surface perspective. Pharmacological reviews. 1995;47(2):331-85. Epub 1995/06/01.
18. Bliss CI. The calculation of microbial assays. Bacteriological reviews. 1956;20(4):243-58. Epub 1956/12/01.
19. Wullaert A, Heyninck K, Beyaert R. Mechanisms of crosstalk between TNF-induced NF-kappaB and JNK activation in hepatocytes. Biochem Pharmacol. 2006;72(9):1090-101. Epub 2006/08/29.
20. Gray-Schopfer VC, Karasarides M, Hayward R, Marais R. Tumor necrosis factor-alpha blocks apoptosis in melanoma cells when BRAF signaling is inhibited. Cancer Res. 2007;67(1):122-9. Epub 2007/01/11.
21. Gray-Schopfer V, Wellbrock C, Marais R. Melanoma biology and new targeted therapy. Nature. 2007;445(7130):851-7. Epub 2007/02/23.
22. Chudnovsky Y, Khavari PA, Adams AE. Melanoma genetics and the development of rational therapeutics. J Clin Invest. 2005;115(4):813-24. Epub 2005/04/21.
23. Pandha HS, Heinemann L, Simpson GR, Melcher A, Prestwich R, Errington F, et al. Synergistic effects of oncolytic reovirus and cisplatin chemotherapy in murine malignant melanoma. Clin Cancer Res. 2009;15(19):6158-66. Epub 2009/09/24.
24. Tawbi HA, Kirkwood JM. Management of metastatic melanoma. Semin Oncol. 2007;34(6):532-45. Epub 2007/12/18.
25. King AJ, Patrick DR, Batorsky RS, Ho ML, Do HT, Zhang SY, et al. Demonstration of a genetic therapeutic index for tumors expressing oncogenic BRAF by the kinase inhibitor SB-590885. Cancer Res. 2006;66(23):11100-5. Epub 2006/12/06.
26. Tsai J, Lee JT, Wang W, Zhang J, Cho H, Mamo S, et al. Discovery of a selective inhibitor of oncogenic B-Raf kinase with potent antimelanoma activity. Proc Natl Acad Sci U S A. 2008;105(8):3041-6. Epub 2008/02/22.
27. Heidorn SJ, Milagre C, Whittaker S, Nourry A, Niculescu-Duvas I, Dhomen N, et al. Kinase-dead BRAF and oncogenic RAS cooperate to drive tumor progression through CRAF. Cell. 2010;140(2):209-21. Epub 2010/02/10.

28. Amaravadi RK, Schuchter LM, McDermott DF, Kramer A, Giles L, Gramlich K, et al. Phase II Trial of Temozolomide and Sorafenib in Advanced Melanoma Patients with or without Brain Metastases. Clin Cancer Res. 2009;15(24):7711-8. Epub 2009/12/10.
29. Maki RG, D'Adamo DR, Keohan ML, Saulle M, Schuetze SM, Undevia SD, et al. Phase II study of sorafenib in patients with metastatic or recurrent sarcomas. J Clin Oncol. 2009;27(19):3133-40. Epub 2009/05/20.
30. Toyoizumi T, Mick R, Abbas AE, Kang EH, Kaiser LR, Molnar-Kimber KL. Combined therapy with chemotherapeutic agents and herpes simplex virus type 1 ICP34.5 mutant (HSV-1716) in human non-small cell lung cancer. Hum Gene Ther. 1999;10(18):3013-29. Epub 1999/12/28.
31. Post DE, Devi NS, Li Z, Brat DJ, Kaur B, Nicholson A, et al. Cancer therapy with a replicating oncolytic adenovirus targeting the hypoxic microenvironment of tumors. Clin Cancer Res. 2004;10(24):8603-12. Epub 2004/12/30.
32. Heinemann L, Simpson GR, Boxall A, Kottke T, Relph KL, Vile R, et al. Synergistic effects of oncolytic reovirus and docetaxel chemotherapy in prostate cancer. BMC Cancer. 2011;11:221. Epub 2011/06/08.
33. Gutermann A, Mayer E, von Dehn-Rothfelser K, Breidenstein C, Weber M, Muench M, et al. Efficacy of oncolytic herpesvirus NV1020 can be enhanced by combination with chemotherapeutics in colon carcinoma cells. Hum Gene Ther. 2006;17(12):1241-53. Epub 2006/11/23.
34. Twigger K, Vidal L, White CL, De Bono JS, Bhide S, Coffey M, et al. Enhanced in vitro and in vivo cytotoxicity of combined reovirus and radiotherapy. Clin Cancer Res. 2008;14(3):912-23. Epub 2008/02/05.
35. Pawlik TM, Nakamura H, Mullen JT, Kasuya H, Yoon SS, Chandrasekhar S, et al. Prodrug bioactivation and oncolysis of diffuse liver metastases by a herpes simplex virus 1 mutant that expresses the CYP2B1 transgene. Cancer. 2002;95(5):1171-81. Epub 2002/09/05.
36. Tyminski E, Leroy S, Terada K, Finkelstein DM, Hyatt JL, Danks MK, et al. Brain tumor oncolysis with replication-conditional herpes simplex virus type 1 expressing the prodrug-activating genes, CYP2B1 and secreted human intestinal carboxylesterase, in combination with cyclophosphamide and irinotecan. Cancer Res. 2005;65(15):6850-7. Epub 2005/08/03.
37. Raki M, Kanerva A, Ristimaki A, Desmond RA, Chen DT, Ranki T, et al. Combination of gemcitabine and Ad5/3-Delta24, a tropism modified conditionally replicating adenovirus, for the treatment of ovarian cancer. Gene Ther. 2005;12(15):1198-205. Epub 2005/04/01.
38. Soares JA, Leite FG, Andrade LG, Torres AA, De Sousa LP, Barcelos LS, et al. Activation of the PI3K/Akt pathway early during vaccinia and cowpox virus infections is required for both host survival and viral replication. J Virol. 2009;83(13):6883-99. Epub 2009/04/24.
39. Wang G, Barrett JW, Stanford M, Werden SJ, Johnston JB, Gao X, et al. Infection of human cancer cells with myxoma virus requires Akt activation via interaction with a viral ankyrin-repeat host range factor. Proc Natl Acad Sci U S A. 2006;103(12):4640-5. Epub 2006/03/16.

40. Moore RJ, Owens DM, Stamp G, Arnott C, Burke F, East N, et al. Mice deficient in tumor necrosis factor-alpha are resistant to skin carcinogenesis (vol 5, pg 828, 1999). Nature Medicine. 1999;5(9):1087-.
41. Beyaert R, Van Loo G, Heyninck K, Vandenabeele P. Signaling to gene activation and cell death by tumor necrosis factor receptors and Fas. Int Rev Cytol. 2002;214:225-72. Epub 2002/03/15.
42. Hayden MS, Ghosh S. Signaling to NF-kappaB. Genes Dev. 2004;18(18):2195-224. Epub 2004/09/17.

Figure Legends

Figure 1: Combined GLV-1h68 and radiation treatment in a panel of melanoma cells lines. Cells were irradiated at 1, 3 and 5 Gy and 6 hours later infected with GLV-1h68 at different MOIs. Cell survival was measured using MTT assays at 72 hours post-infection (A) and synergy assessed using the Bliss Analysis method **(**B). Cell survival was further validated using the SRB assay (C) at 72 hours post-infection. Results are shown from 3 independent experiments. *, $P < 0.05$; **, $P < 0.01$; ***, $P < 0.005$. Clonogenic assays were carried out to assess radiation effect in MeWo, A375 and D04 cell lines. MeWo, A375 and D04 cells were plated at an appropriate seeding density and allowed to attach. 24 hours later, cells were irradiated at 2 and 5 Gy. Colony formation was determined at 10-14 days irradiation and the surviving fractions calculated relative to the control. Data are shown from 2 independent experiments (D). Cells were plated at 5×10^5 in a T25 flask and irradiated at 2 Gy after 24 hours. GLV-1h68 was then infected at a MOI of 0.03. 48 hours later, cells were washed in PBS, trypsinized and counted. An equal number of cells were plated from each treatment group into 6-well plates. 10-14 days later, colony assays were stained with crystal violet (E).

Figure 2: Combined GLV-1h68 and radiation (RT) enhances tumor reduction and survival in ^{V600E}BRAF mutant melanoma in vivo. A375 subcutaneous xenograft tumor models were established in nude mice. A). Mice were either untreated (PBS), irradiated

at 2Gy / fraction for 3 cycles, GLV-1h68 infected at 1×10^4 pfu or combined treatment (2Gy / fraction for 3 cycles + 1×10^4 pfu GLV-1h68. B). Size of tumors were measured for each treatment group. Each bar represents mean ± SE of ten replicate. C). Comparison of mean tumor volumes between treatment groups at serial time points after and including day 45 using a Mann-Whitney U test. There was significant inhibition of tumor growth in the GLV-1h68 and RT combination groups compared with other groups. *, $P < 0.05$; **, $P < 0.01$; ***, $P < 0.005$. D). Kaplan-Meier curve was evaluated for each treatment group to assess the median survival rate. There was significant prolongation of survival in the combination of RT and GLV-1h68 compared with either agent alone**.** **, $P = 0.0099$. E). Immunoblot of caspase 3 cleavage, a biomarker of apoptosis was carried out following homogenization of A375 xenografts following seven days post-treatment from each treatment arm. Three mice from each treatment group were used in this experiment. Equal loading of proteins was assessed by probing for GAPDH. F). Tumor frozen sections were used for tunnel staining immunohistochemistry analysis.

Figure 3: Radiation does not increase GLV-1h68 viral replication. Cells were irradiated at 5 Gy and 6 hours later infected with GLV-1h68. The cells were harvested and the supernatants were collected at 4, 24, 48 and 72 hours post-infection in triplicate. Viral titers were determined by using one-step growth curves (A). Cells were irradiated at 5 Gy and 6 hours later infected with GLV-1h68 at an MOI of 1.0. Standard viral plaque assays were performed to assess viral replication in melanoma cells. Supernatants were collected 48 hours later and total viral titers were quantified by plaque assays on confluent CV-1 cells (B). Cells were also analyzed for the presence of GLV-1h68 using vaccinia virus A21L specific primers (C).

Figure 4: Enhanced cell death following radiation and GLV-1h68 is regulated by the JNK signaling pathways. Phospho kinase array in MeWo and A375 cells to assess how the MAPK family kinases are regulated following RT and GLV-1h68 treatment. MeWo (upper left panel) or A375 (upper right panel) cells were either untreated, GLV-1h68 infected (MOI of 0.1), irradiated (5Gy) or combined (5 Gy + GLV-1h68 at MOI of 0.1) and harvested after 72 hours. Cell lysates were prepared and 0.2mg of total protein applied to phospho kinase arrays, which expressed the MAPK signaling pathway (A). Western blot analysis of phospho-JNK, phospho-p38, and phospho-ERK in untreated, GLV-1h68, RT or RT + GLV-1h68 were validated in MeWo and A375 cells to confirm results from kinase array. Equal loading of proteins was assessed by probing for GAPDH (B). Western analysis to assess JNK activation and cleaved caspase-3, a marker of apoptosis in melanoma cells following irradiation at 5 Gy and GLV-1h68 infection between an MOI of 0-0.25 (MeWo, PMWK, A375 and WM266.4) and MOI of 0.1 (WM1791 and DO4) cells. Equal loading of proteins was assessed by probing for GAPDH (C).

Figure 5: JNK mediates GLV-1h68 and RT enhanced apoptosis in $^{V600D/E}$BRAF mutant melanoma. MeWo [wild-type], A375 [^{V600E}BRAF mutant] and D04 [N -RAS mutant] cells were incubated with 1 μM of JNK inhibitor SP00125 for 4 hours and radiated at 5 Gy and then infected with GLV-1h68 after 6 hours at an MOI of 0.1 (upper panel). or transfected with 5 and 10 nM JNK siRNA or scramble control for 4 hours and then infected with GLV-1h68 at an MOI of 0.1 (lower panel). Cell lysates were assessed for cleaved caspase 3 and phospho-JNK at 72 hours by immunoblotting. Equal loading of proteins was assessed by probing for GAPDH (A). Cell viability was carried out using SRB assay (B). Results are shown from 3 independent experiments. ***, $P < 0.005$. Viral plaques from MeWo and A375 cell lines were stained by β-galactosidase and visualized

microscopically (C) while viral replication was validated using one step growth curve assays (D).

Figure 6: A panel of melanoma cells were incubated with 1 μM of JNK inhibitor SP00125 for 4 hours and radiated at 5 Gy. Cells were then infected with GLV-1h68 after 6 hours at an MOI of 0.1 and lysates probed for cleaved caspase 3 and phospho-JNK at 72 hours by immunoblotting. Equal loading of proteins was assessed by probing for GAPDH (A). The effect of JNK inhibition and radiation on cell viability and viral replication were assessed in WM266.4, Mel624, SKMel28 [$^{V600D/E}$BRAF mutant] and WM17971 [K-RAS mutant] cells using SRB assay (B) and one step growth curve assays (C).

Figure 7: GLV-1h68 treatment results in increased TNF-α secretion and is abrogated following irradiation in a $^{V600D/E}$BRAF mutant melanoma mutant population. A). MeWo, PMWK, A375 and WM266.4 cells were irradiated at 5 Gy and then infected with increasing doses of GLV-1h68. 48 hours later, TNF-α that was secreted into the medium was measured using a TNF-α ELISA. Results are shown from 3 independent experiments. *, $P < 0.05$; ***, $P < 0.005$. B). MeWo and A375 cells were incubated with 1 μM of JNK inhibitor SP00125 or 2ng/ml ml of TNF-α monoclonal antibody (mAb) for 4 hours and radiated at 5 Gy. Cells were then infected with GLV-1h68 after 6 hours at an MOI of 1 (for TNF-α ELISA) or 0.1 (viral plaque assay). TNF-α that was secreted into the medium was measured using a TNF-α ELISA following 72 hours of infection (Left panel). Results are shown from 3 independent experiments. ***, $P < 0.005$. C). Caspase 3 cleavage and JNK activation were measured by Western blotting analysis. Equal loading of proteins was assessed by probing for α-tubulin. D). Cell viability was carried out using

crystal violet assay (D) and SRB assay (E). A Model of $^{V600D/E}$BRAF mutant melanoma cells mediated by JNK following irradiation and GLV-1h68 treatment (F).

Figure 1.

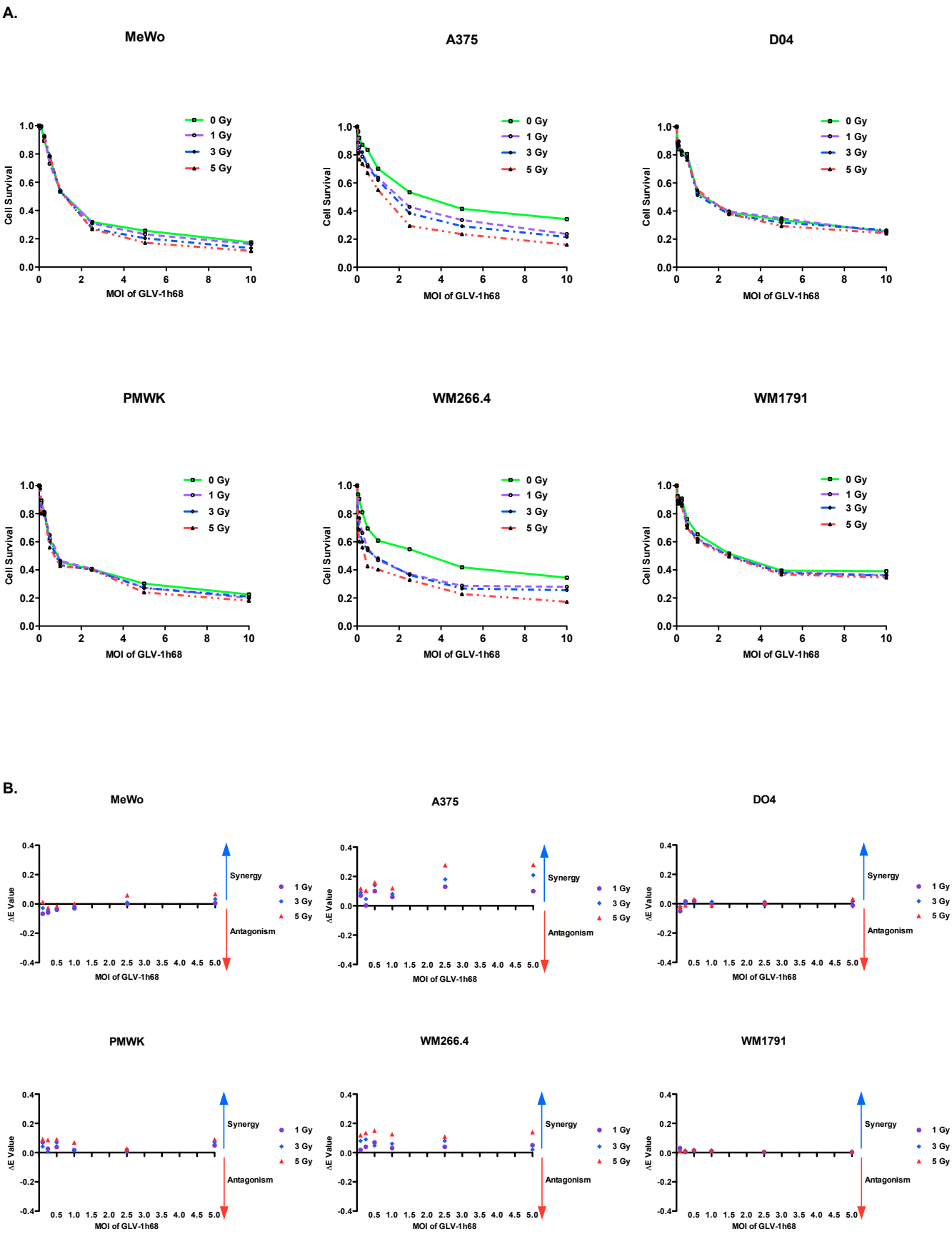
A.
MeWo
A375
D04
PMWK
WM266.4
WM1791
0 Gy
1 Gy
3 Gy
5 Gy
Cell Survival
MOI of GLV-1h68
B.
MeWo
A375
DO4
PMWK
WM266.4
WM1791
ΔE Value
Synergy
Antagonism
1 Gy
3 Gy
5 Gy
MOI of GLV-1h68

Figure 1.

C.

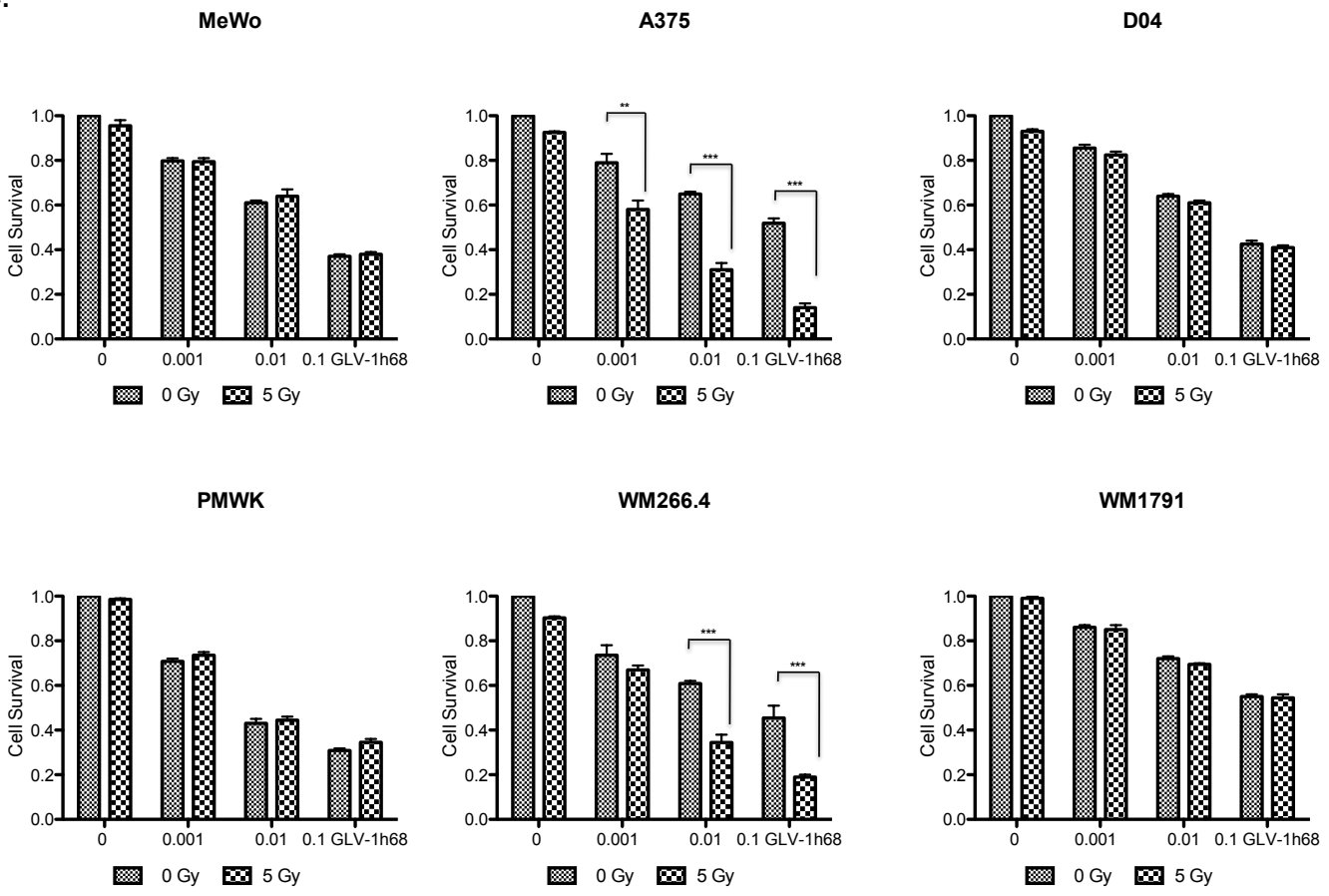
MeWo
A375
D04
PMWK
WM266.4
WM1791
Cell Survival
1.0
0.8
0.6
0.4
0.2
0.0
0
0.001
0.01
0.1 GLV-1h68
0 Gy
5 Gy
**
***
***
***
***

D.

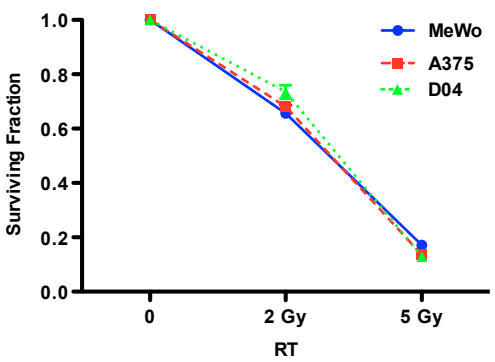
Surviving Fraction
1.0
0.8
0.6
0.4
0.2
0.0
0
2 Gy
5 Gy
RT
MeWo
A375
D04

E.

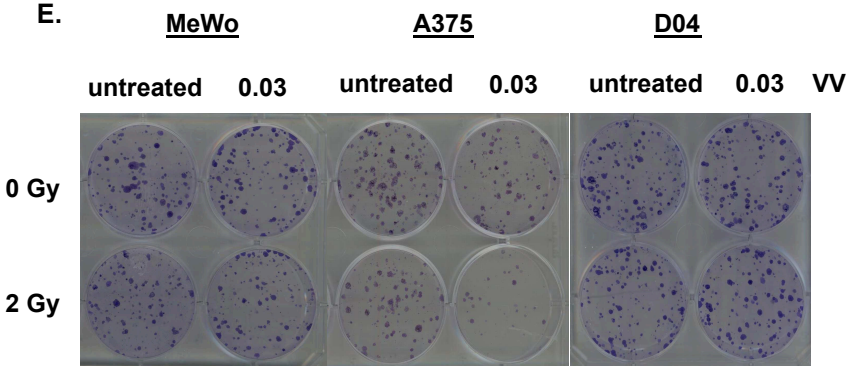
MeWo
A375
D04
untreated
0.03
untreated
0.03
untreated
0.03
VV
0 Gy
2 Gy

Figure 2.

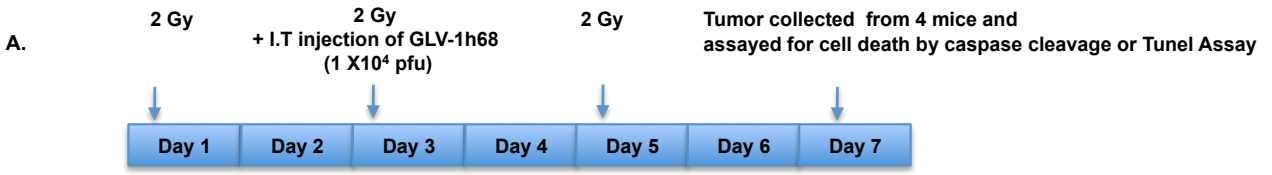
A.
2 Gy
2 Gy
+ I.T injection of GLV-1h68
(1 X10⁴ pfu)
2 Gy
Tumor collected from 4 mice and
assayed for cell death by caspase cleavage or Tunel Assay
Day 1
Day 2
Day 3
Day 4
Day 5
Day 6
Day 7

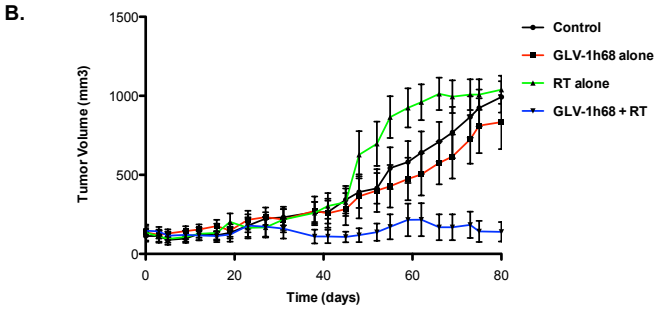
B.
Tumor Volume (mm3)
Time (days)
Control
GLV-1h68 alone
RT alone
GLV-1h68 + RT

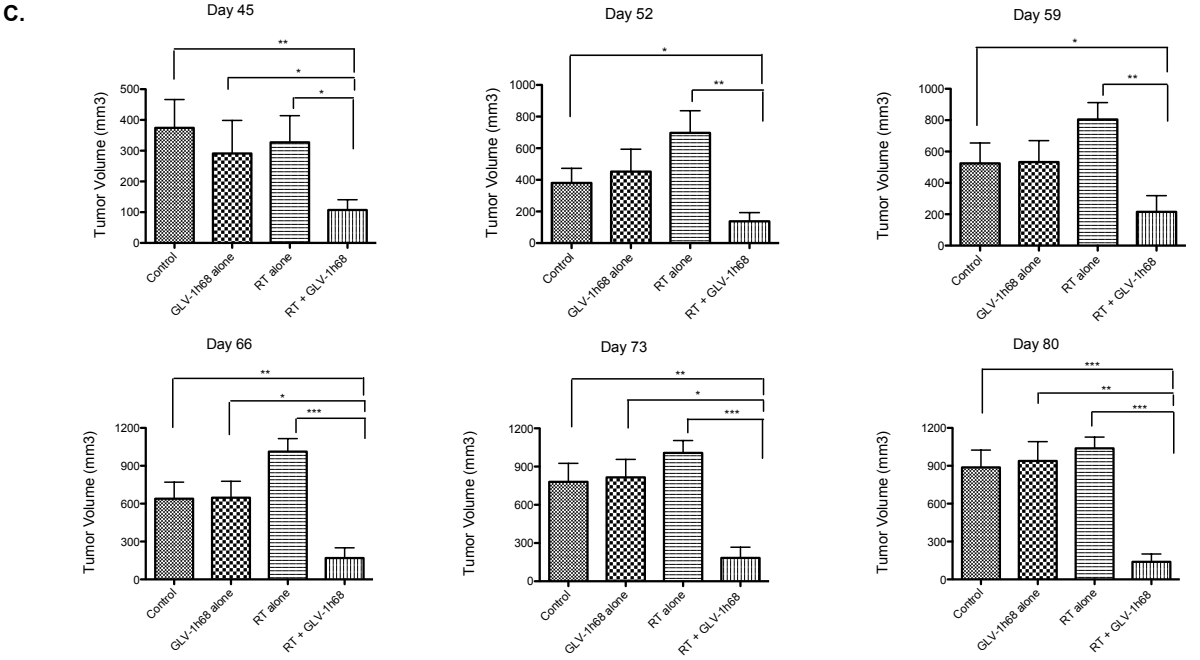
C.
Day 45
Day 52
Day 59
Day 66
Day 73
Day 80
Tumor Volume (mm3)
Control
GLV-1h68 alone
RT alone
RT + GLV-1h68

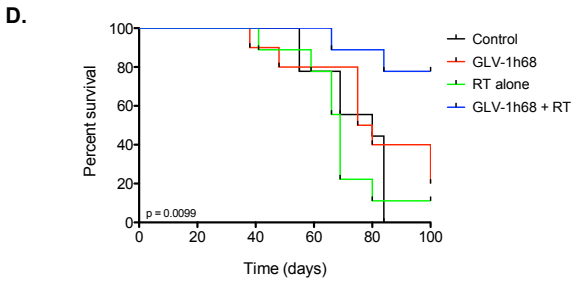
D.
Percent survival
Time (days)
p = 0.0099
Control
GLV-1h68
RT alone
GLV-1h68 + RT

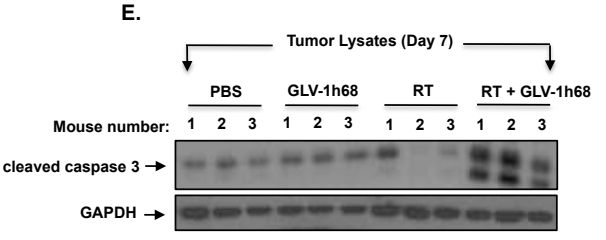
E.
Tumor Lysates (Day 7)
PBS
GLV-1h68
RT
RT + GLV-1h68
Mouse number:
1 2 3 1 2 3 1 2 3 1 2 3
cleaved caspase 3
GAPDH

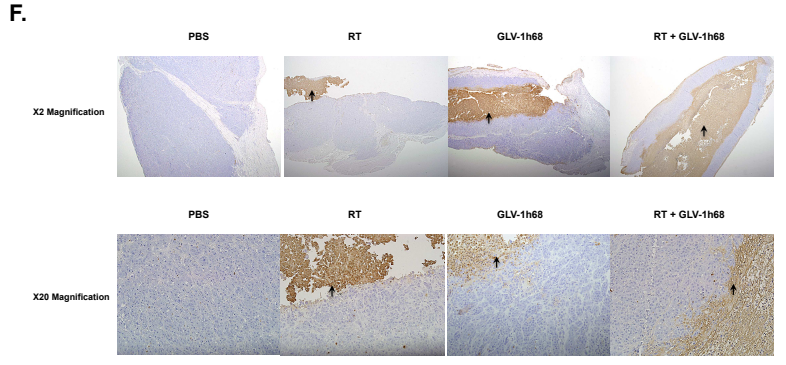
F.
PBS
RT
GLV-1h68
RT + GLV-1h68
X2 Magnification
X20 Magnification

Figure 3

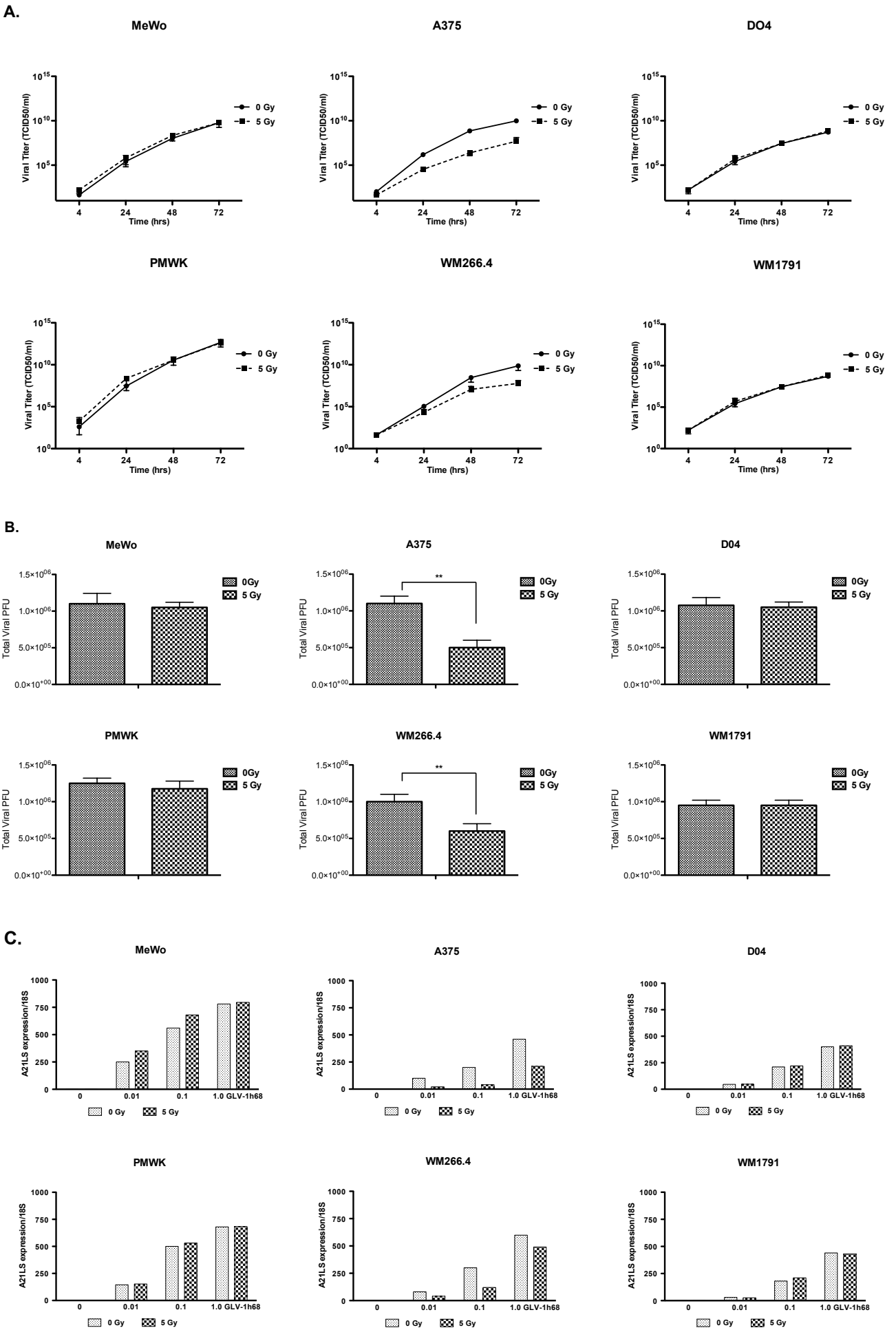
A.
MeWo
A375
DO4
PMWK
WM266.4
WM1791
Viral Titer (TCID50/ml)
Time (hrs)
0 Gy
5 Gy
B.
MeWo
A375
D04
PMWK
WM266.4
WM1791
Total Viral PFU
0Gy
5 Gy
**
C.
MeWo
A375
D04
PMWK
WM266.4
WM1791
A21LS expression/18S
0
0.01
0.1
1.0 GLV-1h68
0 Gy
5 Gy

Figure 4.

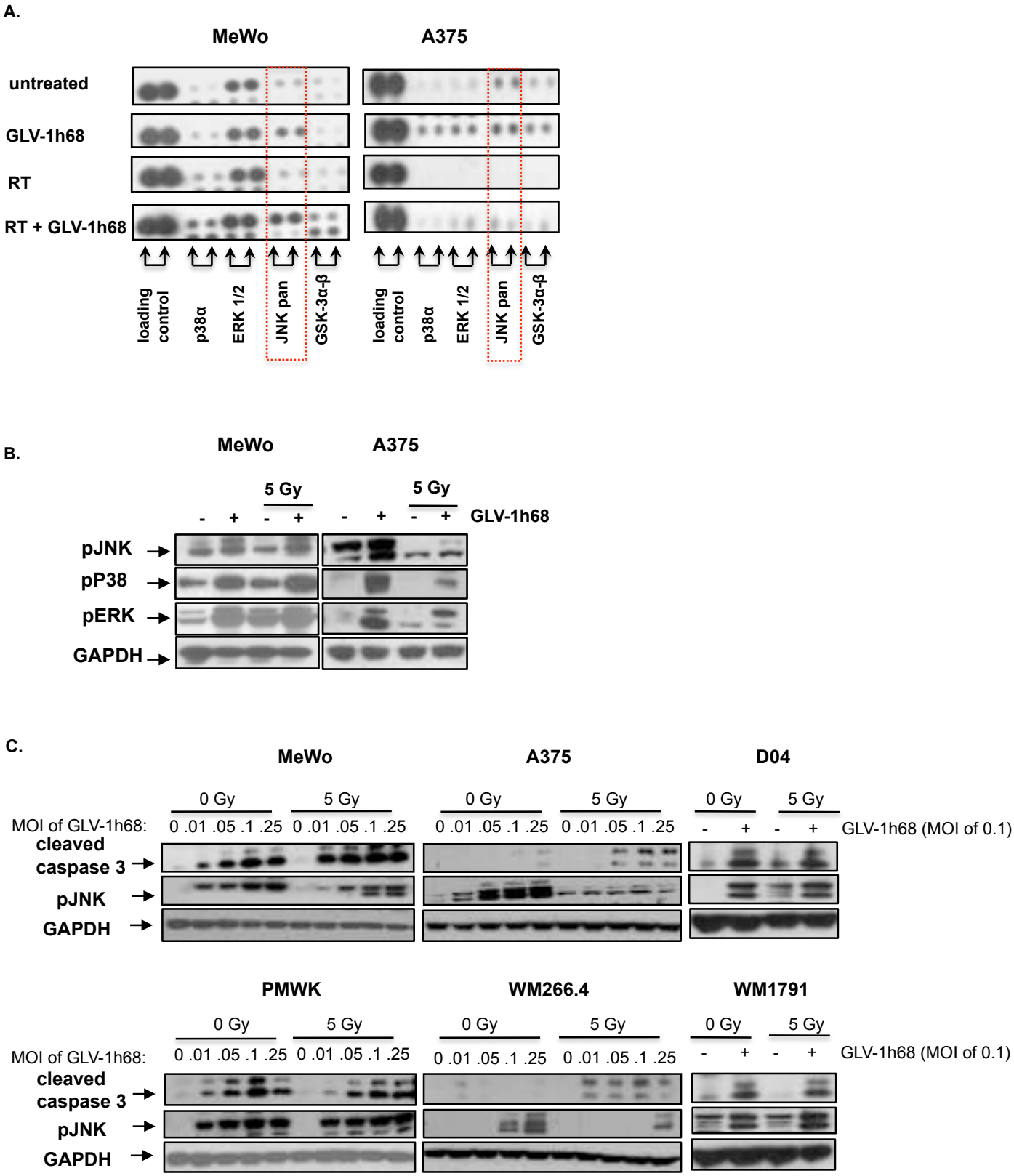
A.
MeWo
A375
untreated
GLV-1h68
RT
RT + GLV-1h68
loading control
p38α
ERK 1/2
JNK pan
GSK-3α-β
B.
MeWo
A375
5 Gy
5 Gy
- + - + - + - + GLV-1h68
pJNK
pP38
pERK
GAPDH
C.
MeWo
A375
D04
0 Gy
5 Gy
MOI of GLV-1h68: 0 .01 .05 .1 .25 0 .01 .05 .1 .25
- + - + GLV-1h68 (MOI of 0.1)
cleaved caspase 3
pJNK
GAPDH
PMWK
WM266.4
WM1791

Figure 5.

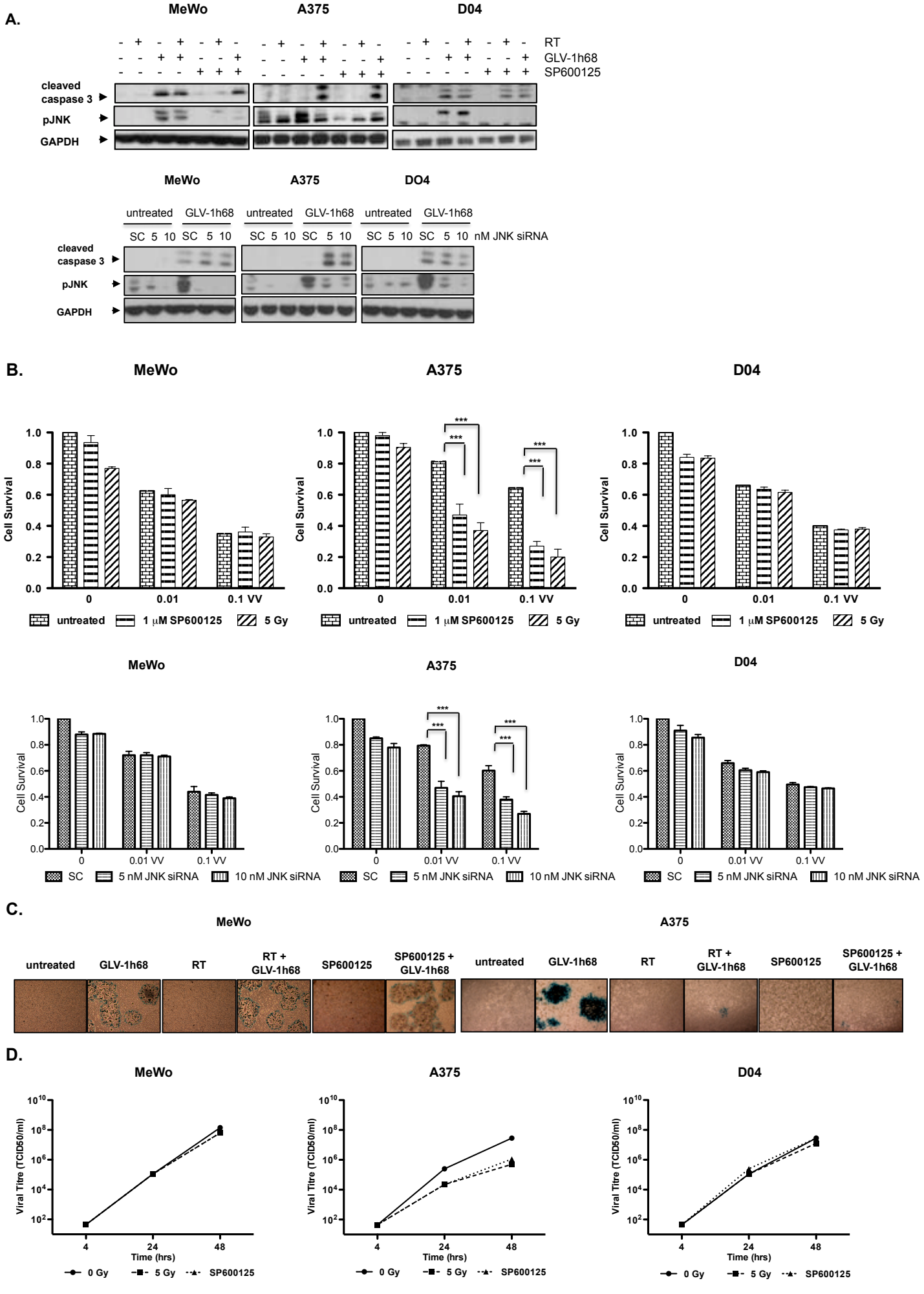
A.
MeWo
A375
D04
RT
GLV-1h68
SP600125
cleaved caspase 3
pJNK
GAPDH
MeWo
A375
DO4
untreated
GLV-1h68
SC 5 10
nM JNK siRNA
B.
MeWo
A375
D04
Cell Survival
0
0.01
0.1 VV
untreated
1 μM SP600125
5 Gy
0.01 VV
SC
5 nM JNK siRNA
10 nM JNK siRNA
C.
MeWo
A375
untreated
GLV-1h68
RT
RT + GLV-1h68
SP600125
SP600125 + GLV-1h68
D.
MeWo
A375
D04
Viral Titre (TCID50/ml)
Time (hrs)
0 Gy
5 Gy
SP600125

Figure 6.

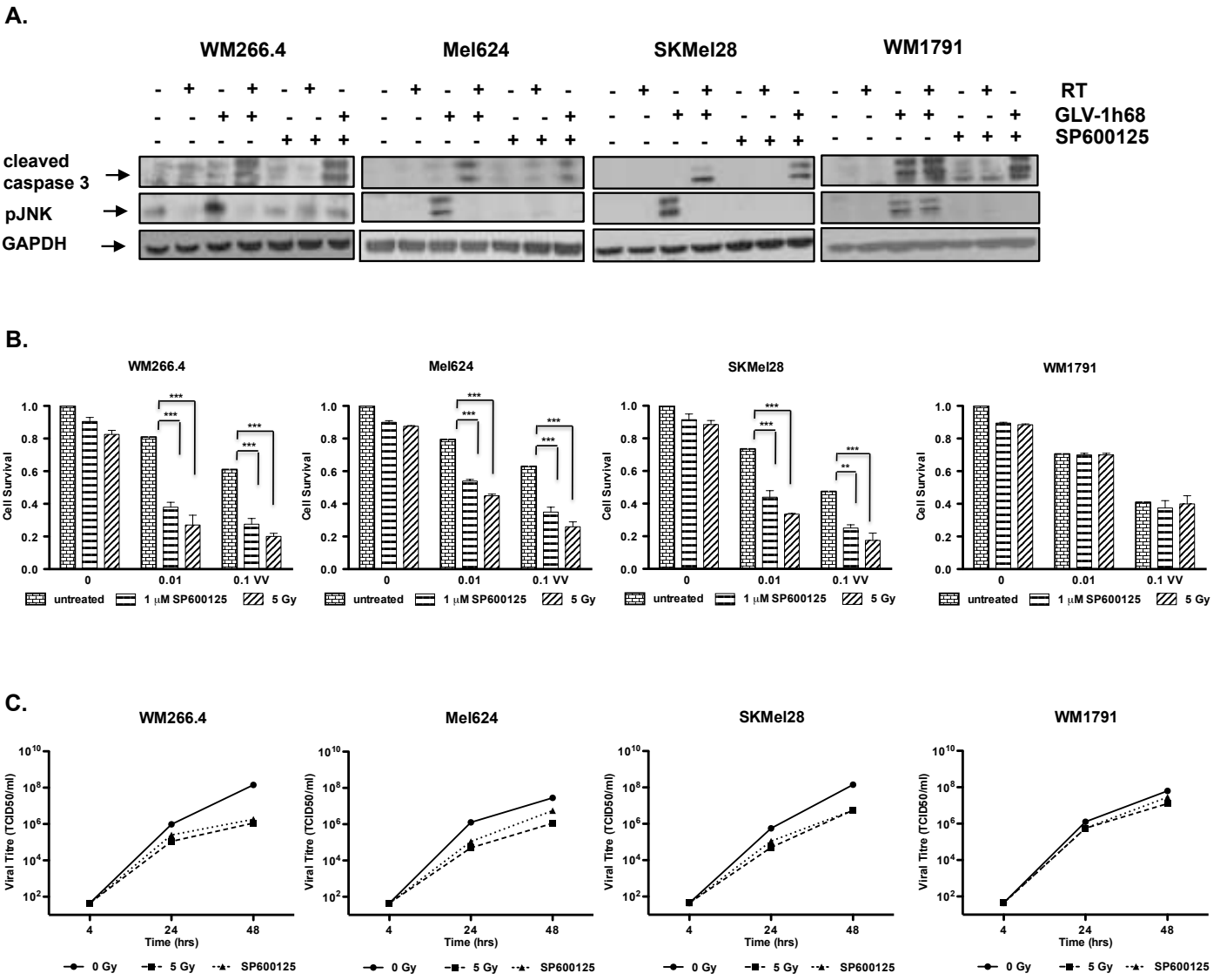
A.
WM266.4
Mel624
SKMel28
WM1791
RT
GLV-1h68
SP600125
cleaved caspase 3
pJNK
GAPDH
B.
WM266.4
Mel624
SKMel28
WM1791
Cell Survival
0
0.01
0.1 VV
untreated
1 μM SP600125
5 Gy
C.
WM266.4
Mel624
SKMel28
WM1791
Viral Titre (TCID50/ml)
Time (hrs)
0 Gy
5 Gy
SP600125

Figure 7.

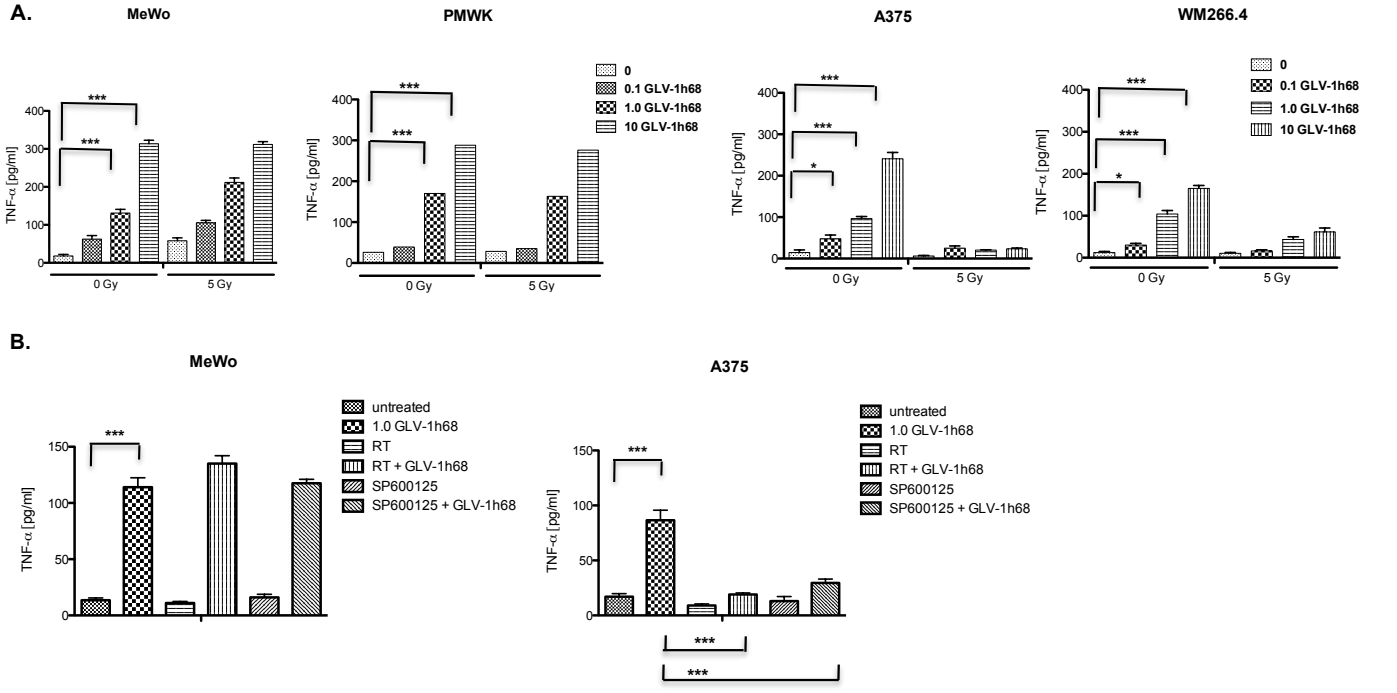
A.
MeWo
PMWK
A375
WM266.4
TNF-α [pg/ml]
0
0.1 GLV-1h68
1.0 GLV-1h68
10 GLV-1h68
0 Gy
5 Gy

B.
MeWo
A375
TNF-α [pg/ml]
untreated
1.0 GLV-1h68
RT
RT + GLV-1h68
SP600125
SP600125 + GLV-1h68

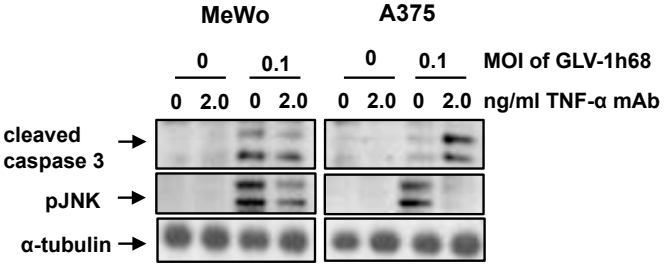
C.
MeWo
A375
MOI of GLV-1h68
ng/ml TNF-α mAb
cleaved caspase 3
pJNK
α-tubulin

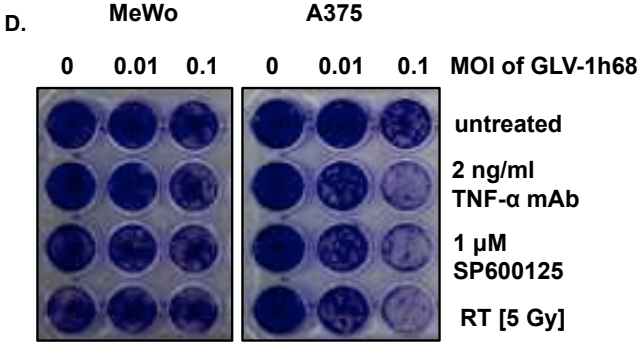
D.
MeWo
A375
MOI of GLV-1h68
untreated
2 ng/ml TNF-α mAb
1 μM SP600125
RT [5 Gy]

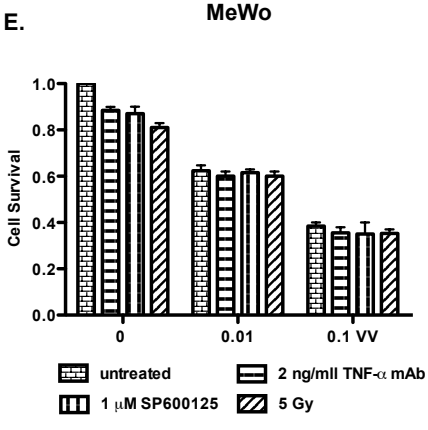
E.
MeWo
Cell Survival
untreated
2 ng/mll TNF-α mAb
1 μM SP600125
5 Gy

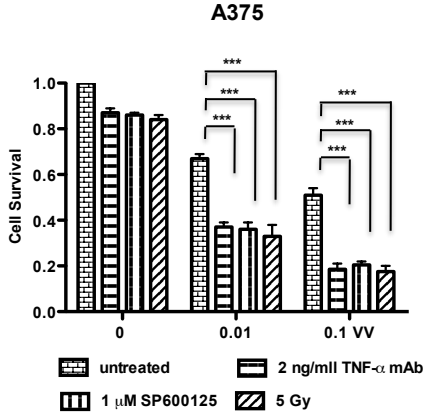
A375
Cell Survival
untreated
2 ng/mll TNF-α mAb
1 μM SP600125
5 Gy

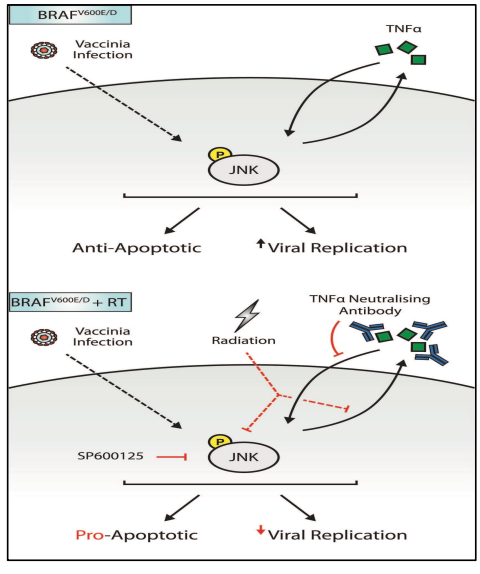
F.
Vaccinia Infection
TNFα
JNK
Anti-Apoptotic
Viral Replication
Radiation
TNFα Neutralising Antibody
SP600125
Pro-Apoptotic